Local Superfluidity at the Nanoscale

B. Kulchytskyy,[1] G. Gervais,[1] and A. Del Maestro[2]

[1] *Department of Physics, McGill University, Montreal, H3A 2T8, Canada*
[2] *Department of Physics, University of Vermont, Burlington, VT 05405, USA*

(Dated: March 29, 2013)

We have performed quantum Monte Carlo simulations measuring the finite size and temperature superfluid response of ^{4}He to the linear and rotational motion of the walls of a nanopore. Within the two-fluid model, the portion of the normal liquid dragged along with the boundaries is dependent on the type of motion and the resulting anisotropic superfluid density saturates far below unity at $T = 0.5$ K. The origin of the saturation is uncovered by computing the spatial distribution of superfluidity, with only the core of the nanopore exhibiting any evidence of phase coherence. The superfluid core displays scaling behavior consistent with Luttinger liquid theory, thereby providing an experimental test for the emergence of a one dimensional quantum liquid.

PACS numbers: 67.25.dr, 02.70.Ss, 05.30.Jp, 67.25.dj

Superfluidity or dissipation-free flow, is rooted in quantum mechanics with the wave function of the entire fluid being described by an emergent global macroscopic phase θ. In ^{4}He, this breaking of gauge symmetry has dramatic consequences for the liquid below the superfluid transition, $T_\lambda \simeq 2.17$ K. It is well established that superfluid helium can flow through extremely narrow constrictions, impenetrable to the normal liquid, with a velocity $\boldsymbol{v}_s = (\hbar/m)\boldsymbol{\nabla}\theta$ limited only by a critical velocity first understood by Landau. In "rotating bucket" experiments, where a container of superfluid is rotated at an angular frequency ω, vortices can be spontaneously created, yielding a non-zero quantum of fluid circulation $\kappa = \oint \boldsymbol{v}_s \cdot d\boldsymbol{r} = \frac{h}{m}W$, where $W \in \mathbb{Z}$ is the topological winding number, equal to the number of vortices within a closed circulation loop. The quantitative details of the superfluid state were first probed in the celebrated Andronikashvili torsional oscillator experiment in 1946 where it was determined that a *superfluid fraction* of the total fluid does not contribute to the classical moment of inertia. This observation led to the development of Tisza's phenomenological two-fluid model where the superfluid state is understood as two intertwined liquids, having normal (ρ_n) and superfluid (ρ_s) components with total density $\rho = \rho_n + \rho_s$.

The superfluid-normal transition in bulk ^{4}He is in the three dimensional ($3d$) XY universality class. As the spatial dimension of the system is reduced, the enhancement of fluctuations suppresses the transition temperature to zero in $2d$ and precludes any long range ordered state in one dimension. It is intriguing to consider how the continuum two-fluid picture holds up in the low dimensional limit where the bosonic helium system should be described by the universal harmonic Luttinger liquid (LL) theory [1] at low energies. Such a correlated liquid is strongly fluctuating with any phase coherence decaying algebraically as a function of distance at $T = 0$ K. Experimental realizations of low dimensional bosonic systems have been achieved in ultra-cold atomic gases [2] at low densities where the interactions are expected to be weak and short ranged, but at higher densities, direct observations of LL behavior are still lacking. Previous experimental work in low-d quantum fluids has focused on superfluid helium confined to porous materials with a radial length scale in the nanometer range, and there is evidence for a new quantum phase occurring at low temperature [3, 4]. Recently, experiments have demonstrated the feasibility of measuring the superflow of helium through nanometer sized holes [5]. The next step will be to systematically decrease the radius of the nanopore, thereby providing a quasi-$1d$ flow geometry in which the superfluid properties of helium can be measured. Unequivocal evidence of LL behavior in ^{4}He filled nanopores will require a detailed understanding of the signatures of low dimensional superfluidity in the crossover regime and we have performed large scale numerical simulations to elucidate this behavior. After providing details of our microscopic model and numerical methods, we present the low temperature superfluid density which we identify as originating from only the Luttinger liquid core region of pores with nanometer radii.

The starting point is a system of helium-4 confined inside a nanopore of radius R and length L formed as a cylindrical cavity in a slab of amorphous silicon nitride. The interactions between helium atoms are modeled via the Aziz potential [6] while confinement is achieved by combining the effects of short range repulsion with the walls of the pore and a long range dispersion force between helium and the surrounding medium [7]. The resulting quantum many-body Hamiltonian can be exactly simulated using continuous space Worm Algorithm (WA) quantum Monte Carlo (QMC) [8]. Within the path integral formulation, this method exploits the quantum-classical isomorphism, performing Metropolis sampling of $(d+1)$-dimensional configurations of bosons that can be visualized as worldlines or trajectories in an imaginary time (τ) direction [9]. For helium at finite temperature, the worldlines obey a periodicity condition in the

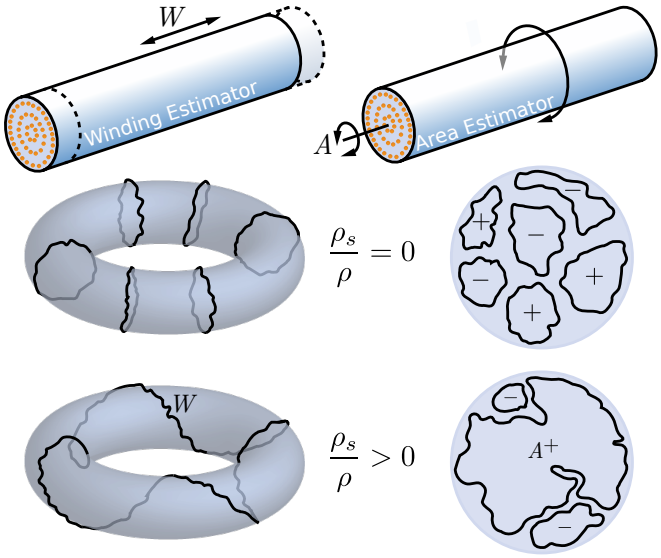

FIG. 1. (color online). The origin of superfluidity in ^{4}He filled nanopores measured by the *winding* (W, left column) and *area* (A, right column) estimators in the path integral representation. At high temperature, helium worldlines are short, containing only single particles and there is no superfluid fraction: $\rho_s/\rho = 0$. As the temperature is lowered, the worldlines may link with each other, winding around periodic boundary conditions in the simulation cell and having a large projected net area perpendicular to the axis of rotation.

additional dimension modulo identical particle permutations, owing to their bosonic symmetry. The superfluid response of the low temperature system is directly linked to the existence and properties of long connected worldline exchange cycles consisting of many individual atoms.

Our simulations employ a fixed chemical potential $\mu/k_{\rm B} = -7.2$ K to ensure helium atoms in pores of $L = 75$ Å and $R = 3.0 - 15.0$ Å are in thermal contact with a bath held at saturated vapor pressure (SVP) for temperatures between $0.5 - 2.25$ K.

In QMC, the superfluid density is measured using linear response theory by considering the effects of boundary motion [10]. Within the two-fluid model, it is supposed that a superfluid fraction ρ_s/ρ will remain stationary while the normal portion ρ_n/ρ will be dragged along with the walls of the container. In the nanopore geometry, two types of motion, depicted in the first row of Fig. 1 are possible: translational motion of the walls along the cylindrical axis and a rotation around it. These two types of response correspond to different measurements in the QMC, related to the geometry and topology of particle worldlines, represented as closed loops due to periodicity in imaginary time. In the case of transverse wall motion, (left column, Fig. 1) we consider a container with periodic boundary conditions along the axis of the pore, and for the purposes of visualization, imagine the volume inside the pore to be mapped onto the surface of a torus. The major circumference of the torus is equal to L while the minor one is $\hbar\beta$ with $\beta = 1/k_{\rm B}T$. In the path integral representation, $W = (1/L)\sum_{i=1}^{N}\int_0^{\hbar\beta} d\tau[dz_i(\tau)/d\tau]$ where $z_i(\tau)$ is the z-component of $\boldsymbol{r}_i(\tau)$, the $(d+1)$-dimensional position of particle i, is equivalent to the number of times the imaginary time trajectories of the N particles wrap around the periodic boundary conditions of the sample. In WA simulations, the imaginary time τ must be discretized and we use $k_{\rm B}\Delta\tau/\hbar = 0.004$ K^{-1} to minimize Trotter error. The resulting superfluid density $\rho_s^{\rm W}$ is related to the variance of the distribution of winding numbers present[9, 10] through a *winding estimator*,

$$\rho_s^{\rm W} = \frac{mL}{\pi R^2\hbar^2\beta}\langle W^2\rangle \tag{1}$$

where m is the mass of a helium atom and $\langle\cdots\rangle$ indicates a QMC average. At high temperature, the helium atoms behave classically, with spatially localized worldlines containing only a single atom. Long exchange cycles are extremely unlikely and so $\langle W^2\rangle = 0$. As the temperature is lowered, the kinetic energy can be reduced by linking worldlines together. Such particle exchanges can be efficiently sampled within the WA using spatially local updates, producing configurations with extended worldlines that wind around the periodic boundary conditions ($\langle W^2\rangle \neq 0$), producing a finite superfluid response.

An alternative approach, equivalent in the $d \geq 3$ thermodynamic limit [11], measures the non-classical response of the fluid to a small rotation. The superfluid fraction $\rho_s^{\rm A}/\rho$ is then equal to the non-classical rotational moment of inertia fraction $(I_{\rm cl} - I)/I_{\rm cl}$ where I is the observed moment of inertia and $I_{\rm cl}$ is the total classical moment of inertia. The superfluid fraction defined in this way can be estimated in the QMC by measuring the worldline area A of closed particle trajectories projected onto a plane perpendicular to the axis of rotation [12] through an *area estimator*,

$$\rho_s^{\rm A} = \frac{4\rho m^2}{\hbar^2\beta I_{\rm cl}}\langle A^2\rangle. \tag{2}$$

For a rotation about the z-axis: $A = (1/2)\sum_{i=1}^{N}\int_0^{\hbar\beta} d\tau\{\boldsymbol{r}_i(\tau) \times [d\boldsymbol{r}_i(\tau)/d\tau]\}_z$. At high temperature, the projected mean squared areas are uncorrelated and $\sqrt{\langle A^2\rangle} \sim \Lambda^2$ where $\Lambda = \sqrt{2\pi\hbar^2\beta/m}$ is the thermal de Broglie wavelength and the resulting superfluid fraction will be vanishingly small for large pores as seen in the right column of Fig. 1. As the temperature is reduced and long exchange cycles become energetically favorable, there is a distribution of finite projected areas and $\rho_s^{\rm A}/\rho > 0$. The caveat to this approach is that angular momentum conservation requires that the dimensions of the simulation cell perpendicular to the axis of rotation do not have periodic boundary conditions. A quantum fluid confined inside a nanopore thus provides a geometry where we can directly compare

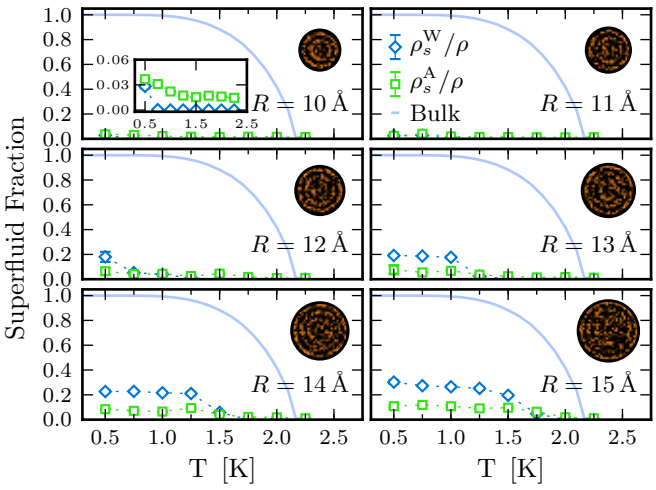

FIG. 2. (color online). A comparison of the superfluid fraction of helium confined inside nanopores with $L = 75$ Å (symbols) measured using the winding number and projected area of particle worldlines with the experimentally measured value [13] (line) for bulk ^{4}He at saturated vapor pressure. Upper right insets show instantaneous quantum Monte Carlo particle configurations projected into the $z = 0$ plane while the lower left inset in the first cell details superfluidity on a finer scale. All panels share the legend shown in the first row.

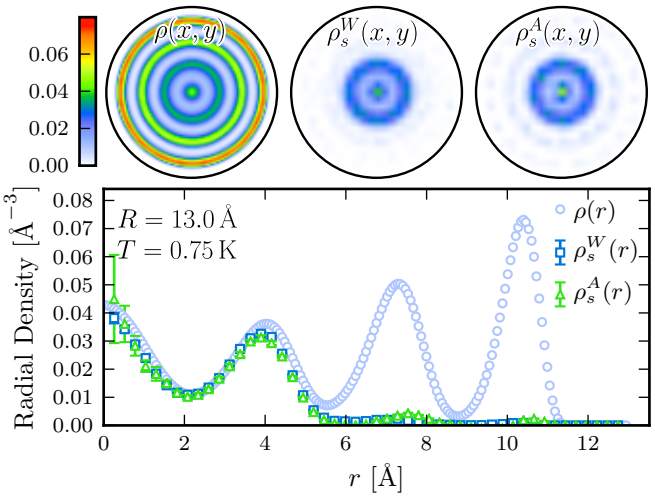

FIG. 3. (color online). The confined superfluid core seen by comparing the particle ρ, winding superfluid and area superfluid number densities measured via quantum Monte Carlo simulations for a $R = 13$ Å radius nanopore of length $L = 75$ Å at $T = 0.75$ K. The first row shows the axially averaged local densities inside the pore while the symbol plot contain an additional angular average.

the two estimators of the superfluid fraction as shown in Fig. 2. The symbols correspond to QMC measurements performed using Eqs. (1) and (2) and the insets in the upper right corners are instantaneous particle configurations projected on the plane $z = 0$. The solid line is the experimentally measured superfluid fraction of ^{4}He at SVP taken from Brooks and Donnelly [13] for comparison. For pores with $R \leq 9$ Å we do not observe any persistent superfluid response above $T = 0.5$ K while for $R \geq 10$ Å, $\rho_s^{W,A}/\rho$ becomes non-zero at a radius dependent onset temperature shifted below the bulk value of T_λ. This is the expected behavior for a quantum fluid constrained inside a porous material where confinement has been shown to reduce T_c and ρ_s/ρ.

The observed superfluid response measured via the winding number is effectively one dimensional, originating from flow along the pore axis, and any non-zero value should be considered a finite size effect that will disappear as $L \to \infty$. Another striking feature distinguishing the nanopore superfluid fraction from that of bulk helium is an apparent saturation at low temperature for both ρ_s^W and ρ_s^A at a value much less than one. A hint at the origin of this behavior can be observed by examining the spatial configurations inside the pore in Fig. 2. The interplay of interactions between helium atoms as well as with the surrounding amorphous Si_3N_4 leads to states exhibiting a series of cylindrical shells [14, 15], equivalent to the formation of thin film layers of helium observed on $2d$ substrates including silicate [16].

The competition between the tendency of bosons to delocalize at low T and the strong geometrical confinement effects in the pore can be investigated by measuring the local contribution of the superfluid density. This was achieved by histogramming the radial r-dependence of the winding number [17] or path area [18]

$$\rho_s^W(r) = \frac{mL^2}{\hbar^2\beta}\langle W \cdot W(r)\rangle \tag{3}$$

$$\rho_s^A(r) = \frac{4mL^2}{\hbar^2 I_{\rm cl}(r)}\langle A \cdot A(r)\rangle \tag{4}$$

with W and A the full pore values defined above while $W(r) = (2\pi r L^2)^{-1}\sum_{i=1}^N \int_0^{\hbar\beta} d\tau [dz_i(\tau)/d\tau]\delta(r - r_i^\perp(\tau))$ and $A(r) = (4\pi r L)^{-1}\sum_{i=1}^N \int_0^{\hbar\beta} d\tau \{\boldsymbol{r}_i(\tau) \times [d\boldsymbol{r}_i(\tau)/d\tau]\}_z \delta(r - r_i^\perp(\tau))$ where $I_{\rm cl}(r) = mr^2$ is the classical moment inertia of a single helium atom and $r_i^\perp(\tau) = \sqrt{x_i^2(\tau) + y_i^2(\tau)}$. A comparison of the average particle number density with the two types of local superfluid density can be seen in Fig. 3 for a nanopore with $R = 13$ Å, $L = 75$ Å at $T = 0.75$ K. The upper panels have been averaged over the z-axis while the lower plot contains the fully cylindrically symmetric radial values defined in Eqs. (3) and (4). The saturation of the total superfluid density seen in Fig 2 can now be immediately understood in terms of a spatial "phase" separation where only the inner volume of the pore contains superfluid helium while the outer shells remain classical, adhering to the walls. The results are qualitatively similar for $R = 10 - 15$ Å with the two outermost shells

making a negligible contribution to the superfluid density. The local superfluid estimators are nearly identical while their total values can differ by a factor of two. This presents no paradox due to their different normalizations: $\rho_s^{\rm W}/\rho \equiv (2\pi L/N)\int_0^R rdr\rho_s^{\rm W}(r)$, $\rho_s^{\rm A}/\rho \equiv (2\pi Lm/I_{\rm cl})\int_0^R rdr[r^2\rho_s^{\rm A}(r)]$ needed to account for local contributions to the classical moment of inertia present in inhomogeneous fluids $I_{\rm cl} \equiv 2\pi Lm\int_0^R rdr[r^2\rho(r)]$.

The core region exhibiting a non-zero superfluid response is nearly one dimensional, having a radius of $R \lesssim 6$ Å. In $d = 1$, fluctuations preclude the existence of any long range superfluid order, and instead, the helium system should be described at lowest order, by the linear quantum hydrodynamics of Luttinger liquid (LL) theory [1] with effective Hamiltonian $H = (\hbar v/2\pi)\int_0^L dz[(\partial_z\phi)^2/K + K(\partial_z\theta)^2]$. The phases $\phi(z)$ and $\theta(z)$ are defined in terms of the second quantized helium field operator $\psi^\dagger(z) \sim \sqrt{\partial_z\theta(z)}e^{i\phi(z)}$ such that $[\phi(z), \partial_{z'}\theta(z')] = i\pi\delta(z-z')$. Its low energy modes have dispersion $\varepsilon(k) = \hbar vk$ and the value of the Luttinger parameter K tunes the system between algebraic superfluid ($K \ll 1$) or solid ($K \gg 1$) order. For a real physical system, the velocities $v_J \equiv v/K$ and $v_N \equiv vK$ can be related to the microscopic parameters of the underling many-body Hamiltonian. By comparing the predictions of harmonic LL theory, derived from the grand partition function $\mathcal{Z} = {\rm Tr}\exp[-\beta(H-\mu N)]$ with the measurements from finite temperature QMC simulations, v_J and v_N can be determined. For quasi-1d helium confined inside nanopores with $R < 3$ Å, this has already been accomplished [19] but for larger radius pores, required the use of an *ad hoc* cutoff radius when analyzing QMC data. The physical origin of this cutoff is now fully understood as the radius of the superfluid core and we expect it to be described by LL theory[20]:

$$\frac{\rho_s^W}{\rho_c} = 1 - \frac{\pi\hbar\beta v_J}{L}\left|\frac{\theta_3''\left(0, e^{-2\pi\hbar\beta v_J/L}\right)}{\theta_3\left(0, e^{-2\pi\hbar\beta v_J/L}\right)}\right| \qquad (5)$$

where $\theta_3(z,q)$ is a Jacobi theta function with $\theta_3''(z,q) \equiv \partial_z^2\theta_3(z,q)$ and $\rho_c = (N_c/N)\rho$ where N_c is the number of atoms in the core. For each radius, we have performed a rescaling of the total superfluid response displayed in Fig. 2 and determined the velocity $v_J(R)$ through fitting, that yields the best collapse of all low temperature data onto Eq. (5). The results are displayed in Fig. 4 where the temperature scaling of the nanopore superfluidity is consistent with Luttinger liquid theory.

Much remains to be done, including a confirmation of the predicted pore length scaling of $\rho_s^{\rm W}/\rho$. In addition, it seems natural to contemplate the effects of disorder, surely present in the pore walls, as well as the introduction of fermionic ^{3}He which may strongly alter superfluidity as bosonic exchanges will be suppressed in 1d.

In conclusion, for pores with $R = 1 - 1.5$ nm we have observed a finite and anisotropic superfluid response

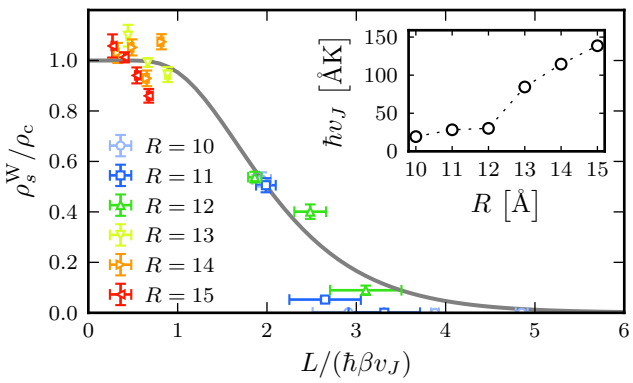

FIG. 4. (color online). The superfluid fraction of the core of nanopores for varying radii which can be collapsed onto the universal prediction from Luttinger liquid theory. The inset shows the extracted value of the phase velocity $\hbar v_J$ obtained by fitting to the winding number estimator for each radius.

above $T = 0.5$ K, with a magnitude that is dependent on whether linear or rotational motion of the cylinder is considered. The difference is large and arises from the absence of any classical moment of inertia in the truly 1d limit where flow is still possible. Experiments probing this breakdown of the naive two-fluid picture could be performed by comparing the superfluid fraction measured by capillary flow and a nanoscale Andronikashvili torsional oscillator. Our results also indicate that when the radii of nanopores becomes sufficiently small, the superfluid fraction may exhibit plateaus, increasing in steps, due to the classical sticking of wetting layers near the pore walls. This is in stark contrast to the usual smooth temperature dependence of ρ_s/ρ observed for bulk ^{4}He and could provide a signature of the crossover to 1d behavior. If the fraction of atoms adhering to the nanopores walls could be discerned, possibly by comparing flow rates at high and low temperature, an examination of the finite size and temperature scaling of the superfluid density could confirm that confined low-dimensional helium is a Luttinger liquid.

We acknowledge financial support from the University of Vermont, NSERC (Canada), FQNRT (Québec), and the Canadian Institute for Advanced Research (CIFAR). This research has been enabled by the use of computational resources provided by the Vermont Advanced Computing Core supported by NASA (NNX-08AO96G), WestGrid, SHARCNET and Compute/Calcul Canada.

[1] F. D. M. Haldane, Phys. Rev. Lett. **47**, 1840 (1981).
[2] M. Cazalilla, R. Citro, T. Giamarchi, E. Orignac, and M. Rigol, Rev. Mod. Phys. **83**, 1405 (2011).
[3] K. Yamamoto, Y. Shibayama, and K. Shirahama, Phys.

Rev. Lett. **100**, 195301 (2008).
[4] J. Taniguchi, R. Fujii, and M. Suzuki, Phys. Rev. B **84**, 134511 (2011).
[5] M. Savard, G. Dauphinais, and G. Gervais, Phys. Rev. Lett. **107**, 254501 (2011).
[6] R. A. Aziz, V. P. S. Nain, J. S. Carley, W. L. Taylor, and G. T. McConville, J. Chem. Phys. **70**, 4330 (1979).
[7] G. J. Tjatjopoulos, D. L. Feke, and J. A. Mann, J. Phys. Chem. **92**, 4006 (1988).
[8] M. Boninsegni, N. V. Prokofev, and B. V. Svistunov, Phys. Rev. E **74**, 036701 (2006).
[9] D. M. Ceperley, Rev. Mod. Phys. **67**, 279 (1995).
[10] E. Pollock and D. M. Ceperley, Phys. Rev. B **36**, 8343 (1987).
[11] N. Prokof'ev and B. Svistunov, Phys. Rev. B **61**, 11282 (2000).
[12] P. Sindzingre, M. L. Klein, and D. M. Ceperley, Phys. Rev. Lett. **63**, 1601 (1989).
[13] J. S. Brooks and R. J. Donnelly, J. Phys. Chem. Ref. Data **6**, 51 (1977).
[14] E. S. Hernández, J. Low Temp. Phys. **162**, 583 (2010).
[15] M. Rossi, D. Galli, and L. Reatto, Phys. Rev. B **72** (2005); M. Rossi, D. E. Galli, and L. Reatto, J. Low Temp. Phys. **146**, 95 (2006).
[16] M. Boninsegni, J. Low Temp. Phys. **159**, 441 (2010).
[17] S. Khairallah and D. M. Ceperley, Phys. Rev. Lett. **95**, 185301 (2005).
[18] Y. Kwon, F. Paesani, and K. Whaley, Phys. Rev. B **74**, 174522 (2006).
[19] A. Del Maestro, M. Boninsegni, and I. Affleck, Phys. Rev. Lett. **106**, 105303 (2011).
[20] A. Del Maestro and I. Affleck, Phys. Rev. B **82**, 060515(R) (2010).